P- ISSN 1991-8941 E-ISSN 2706-6703
2025,(19), (01): 226 – 232

Journal of University of Anbar for Pure Science (JUAPS) Open Access

Effect of the back contact work function on the performance of Al0.1Ga0.9N/CdS/Si solar cell

Bashar M. Salih*, Asmiet Ramizy

Department of Physics, College of Science, University of Anbar, Anbar, IRAQ
alrawi.bashar1@uoanbar.edu.iq

ARTICLE INFO
Received: 03 / 10 /2024
Accepted: 28/ 10 /2024
Available online: 20/ 06 /2025

DOI: 10.37652/juaps.2024.154021.1324

Keywords:
AlGaN; Solar Cells; work function; Pulsed laser deposition.

ABSTRACT

In the first phase of this study, a layer of cadmium sulfide (CdS) and a layer of aluminum–gallium nitride (Al0.1GaN0.9, 10% AlN with 70% GaN) were deposited on a silicon substrate by using a pulsed laser deposition method. Some physical properties of the prepared films of Al0.1GaN0.9 and CdS were studied. Photoluminescence spectra revealed emission peaks at 471 nm for the CdS layer and 339 nm for AlGaN. The energy bandgap of the CdS layer was 2.63 eV, whereas the bandgap of the AlGaN samples was 3.66 eV. The I–V curve measurements of Al0.1GaN0.9 showed that the barrier height (ΦB) was 0.57 eV, while the electron affinity value was 4.63 eV. In the second phase of this study, the results of the experimental study in a computer simulation were used to assess the effect of the back contact work function on the performance of an AlGaN/CdS/Si solar cell. The increase in the back contact work function improved Jsc and Voc values, enhancing efficiency. In particular, the efficiency of the solar cell significantly increased, reaching 18.92% at a metal work function of ≈5.2 eV.

Introduction

Several nations struggle to provide steady, economical, and environmentally safe electricity [1]. Solar energy and other renewable energy sources are appropriate for supplying these needs. Using renewable energy sources, such as solar cells, can help meet the need for energy and lessen the environmental harm of using fossil fuels [2]. Through the photovoltaic effect, a solar cell composed of semiconductor materials directly transforms light energy into electrical energy by utilizing the p–n junction, a material with electrical properties that change in response to daylight [3].

Gallium nitride (GaN), with a bandgap of 3.4 eV, is an important material used in the fabrication of high-power and high-frequency photovoltaic devices owing to its excellent properties. Its most valuable properties are high saturated electron drift velocity, high breakdown field, and high electron mobility equivalent to that of silicon [4, 5]. Its emission wavelength is 365 nm, which is in the near-ultraviolet (UV) region.

Aluminum nitride (AlN) belongs to the III-N group. Like GaN, AlN is a semiconductor with a direct bandgap energy of 6.2 eV, the highest known energy gap in semiconductor materials, and has a hexagonal crystal structure. AlN emits an electromagnetic spectrum in the UV region, with a wavelength of about 210 nm, the shortest value among semiconductors, which makes it highly interesting for applications such as deep-UV light-emitting diodes and laser diodes; it is a material with exceptional stability at high temperatures [6]. AlN thin films are widely employed in optical and engineering applications [7, 8]. GaN and AlN have the same structures but different lattice parameters as a result of the difference in ionic radius of Ga and Al ions (the difference in size for substitution occupation is Al^{3+} =0.53 Å and Ga^{3+} =0.61 Å); therefore, they are used to make AlGaN alloys [9].

AlGaN ternary alloys demonstrate exceptional electrical characteristics, such as thermal and electrical conductivity, robust breakdown fields, high peak and saturation velocities, and resistance to heat and radiation

*Corresponding author at : Department of Physics, College of Science, University of Anbar, Anbar, Iraq
ORCID:https:// https://orcid.org/0000-0000-0000-0000 ,
Tel: +964 7829141620
Email: alrawi.bashar1@uoanbar.edu.iq

changes. AlxGa1-xN materials possess a direct and spacious range gap energy, making them remarkably well suited for solar-blind photodetectors that function in the UV region. The bandgap ranges from 6.2 eV for AlN to 3.4 eV for GaN [10].

In creating an AlxGa(1-x)N alloy (where x specifies the fraction of substituted aluminum), AlN is mixed with GaN to achieve a variable bandgap over a wide range [11]. Through controlling the percentage of Al and Ga in AlGaN alloys, the band edge of the electromagnetic spectrum changes from 365 nm to 200 nm [12, 13]. These alloys may contribute to increasing the efficiency of solar cells by absorbing the UV portion of sunlight.

Solar Cell Capacitance Simulator (SCAPS)-1D

SCAPS, a program developed at Gent University, designs and simulates polycrystalline thin-film solar cells [14]. According to Reference [15], the photovoltaic research community has access to it. Numerical analysis with SCAPS is based on solving three basic equations for semiconductors, namely, Poisson's equation, the continuity equation, and the carrier transport equations for electrons and holes, to study the performance of solar cells simulated under different conditions. These equations can be expressed as follows [16, 17]:

$$\frac{d^2\delta(x)}{dx^2} = \frac{e}{\varepsilon_\circ \varepsilon_r}\left[p(x) + n(x) + n_b^+ - n_c^- + \alpha_p + \alpha_n\right] \qquad (1)$$

where $n(x)$, $p(x)$, δ, e, $\varepsilon_\circ$, ε_r, n_b^+, n_c^-, α_p, and α_n are the concentrations of electrons and holes, electrostatic potential, electrical charge, vacuum permittivity, relative permittivity, charged impurities of the donor, charged impurities of the acceptor, hole distribution, and electron distribution, respectively

$$\frac{dJ_n}{dx} = \beta - Z$$

$$\frac{dJ_p}{dx} = \beta - Z$$

where β is the rate of generation, and Z is the rate of recombination.

$$Jn = q\mu nn\epsilon + qDn\partial n$$

$$Jp = q\mu pp\epsilon - qDp\partial p$$

Jn and Jp are the current densities for electrons and holes, respectively; μn and μp refer the mobility of carriers; Dn and Dp are the diffusion coefficients of electrons and holes, respectively, from the Einstein relationship.

On the basis of the experimental results included in this research and previous experimental results, the SCAPS program was used to study the effect of back contact work function on the performance of an $Al_{0.1}Ga_{0.9}N$/cadmium sulfide (CdS)/Si solar cell.

Experimental Work

For determining some important parameters of the solar cell layers targeted in this study, CdS powder was deposited on a Si substrate using a vacuum thermal evaporation system. Thermal evaporation was performed by resistive heating using a high-current power source.

AlGaN was also deposited on a Si substrate via a pulsed laser deposition system. AlN and GaN targets were prepared from 0.3 g of AlN powder and 2.7 g of GaN powder from Sigma-Aldrich Company to obtain Al (10%): Ga (90%)N with a diameter of 1.5 cm, a thickness of 0.5 cm, and a weight of 3 g. These targets were ablated using a Nd-YAG laser with a wavelength of 532 nm, an energy of 180 J, and a laser pulse number of 600.

Energy gap of prepared films:

Photoluminescence (PL) spectra were used to determine the energy gap (Eg) of the prepared films. The PL spectra of films show a luminesce peak at 471 nm for CdS (Figure 1) and at 339 nm for AlGaN (Figure 2). The energy gap of CdS and AlGaN was determined to be 2.63 and 3.66 eV, respectively, as shown in Table 1.

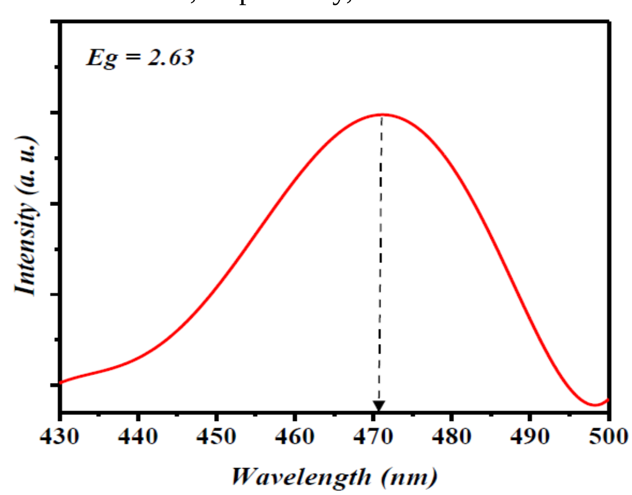

Figure 1. PL emission spectrum for the CdS layer.

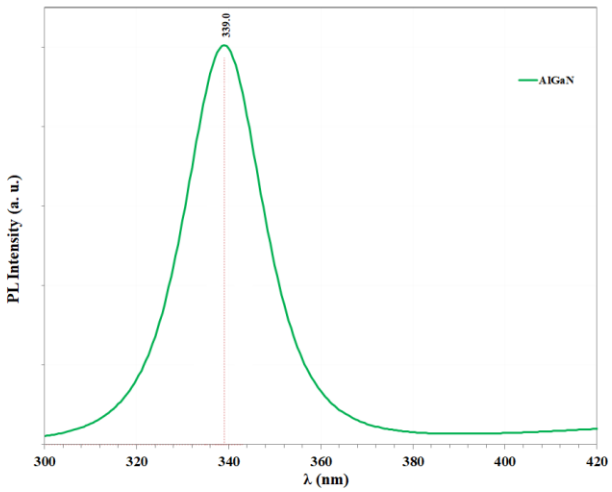

Figure 2. PL emission spectrum for the AlGaN layer.

Table 1. Emission wavelengths and energy gaps of CdS and AlGaN

Name of sample	Wavelength (nm)	Energy gap (eV)
CdS layer	471	2.63
AlGaN layer	339	3.66

I–V Characteristics

For studying the I–V characteristics of the prepared AlGaN films, gold electrodes were deposited on AlGaN films by using a thermal evaporation deposition system to obtain a Schottky diode. The measures of the I–V curve were used to determine the transmission mechanism and electrical parameters of the samples, such as barrier height (ΦB), ideality factor (n), and series resistance (R), on the basis of the method of Cheung, S. and N.J.A.p.l. Cheung [18]. Equation 1 was used to determine electron affinity (χ) as follows [19]:

$$\chi = \varphi_M - \varphi_B$$

where φ_M represents the metal work function. The saturation current values, ΦB, n, and R are listed in Table 2.

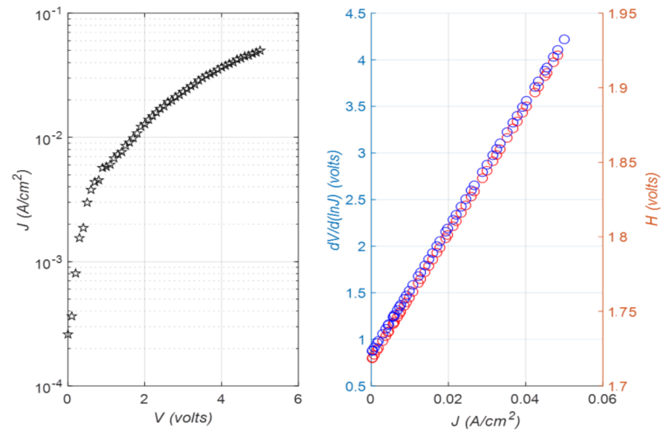

Figure 3. Forward current and the relation between d(V)/d(lnJ) and H function versus J of a Au/Al0.1Ga0.9N Schottky connection.

Table 2. Ideality factor, saturation current, series resistance, barrier height, and electron affinity of AlGaN

Sample	Ideality factor (n)	Saturation current Is (mA)	Series resistance Rs (ohm)	Barrier height φ_B(eV)	Electron affinity χ (eV)
$Al_{0.1}Ga_{0.9}N$	3.011	0.00026	42.011	0.57	4.63

Simulation of solar cells

A numerical analysis with SCAPS (version 3.3.10) software was performed to study the effect of the back contact work function on the electrical measurements of an AlGaN/CdS/Si solar cell. Measurements included open-circuit voltage (Voc), short-circuit current density (Jsc), fill factor (FF%), efficiency percentage (η), and energy band structure. All measurements were obtained at 300 K operating temperature under light conditions of 300–1300 nm.

The main parameters for device installation for solar cell simulation are shown in Table **3**. These parameters were obtained as shown below:

- For the Si layer, parameters from previous studies and the database installed in the program were adopted.
- For the CdS and AlGaN layers, parameters were obtained through an experimental study.

Table 3. Main parameters for device installation for solar cell simulation [20, 21]

Parameter	Symbol (unit)	Si	CdS	$Al_{0.1}Ga_{0.9}N$
Thickness	W(nm)	**300 µm**	**116**	**984**
Bandgap	Eg (eV)	**1.12**	**2.63**	**3.66**

Electron affinity	χ (eV)	**4.5**	**4.2**	**4.63**
Dielectric permittivity	ϵ_r	**11.9**	**10**	**9.45**
C.B density of state	N_c (cm^{-3})	**2.80E+19**	**2.20E+18**	**4.85-E+14**
V.B density of state	N_V (cm^{-3})	**1.04E+19**	**1.80E+19**	**1.00E+12**
Electron thermal velocity	V_n (cm/s)	**1.00E+07**	**1.00E+07**	**1.00E+07**
Hole thermal velocity	V_p (cm/s)	**1.00E+07**	**1.00E+07**	**1.00E+07**
Electron mobility	µn (cm^2/V.S)	**1.50E+03**	**4.97 E+02**	**1.23E+03**
Hole mobility	µp (cm^2/V.S)	**4.50E+03**	**4.00 E+02**	**1.12E+03**
Donor concentration	ND (1/cm^3)	**1E+19**	**15.9E+14**	**4.85E+14**
Acceptor concentration	NA (1/cm^3)	**1.00E+16**	**0**	**0**

Results and discussion

This section discusses the effect of the work function of the back contact on the performance of solar cells. Figure (4) illustrates J_{sc} variation with the back contact work function (Φ_m). When the work function values increase, J_{sc} shows a sudden rise at 4.5 eV. Then, J_{sc} value becomes almost stable when the work function is greater than 5 eV up to 6 eV.

According to the electron affinity (χ) for the p-type Si wafer (4.5 eV) and its bandgap (1.12 eV), for forming an ohmic contact that facilitates hole extraction, the metal work function (Φ_m) should be greater than the effective work function of the p-type silicon (Φ_p), which is given by

$$\Phi_P = \chi + \frac{E_g}{2} = 4.5\ eV + \frac{1.12\ eV}{2} = 5.06\ eV$$

Thus, the metal work function (Φ_m) should be greater than 5.06 eV. Au, Pt, and Pd are examples of suitable metals. This selection ensures the efficient transportation of charge carriers and enhances the overall performance of the solar cell. A low work function of the back contact obstructs charge carrier transport, leading to a marked decrease in the current density.

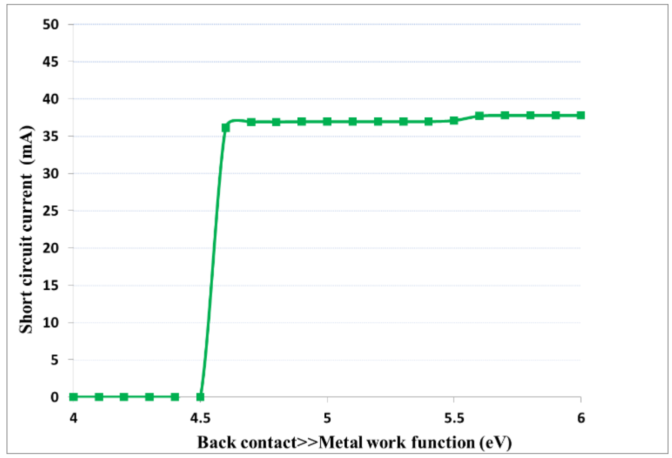

Figure 4. Effect of the back contact work function on Jsc of the AlGaN/CdS/Si solar cell

Figure (5) shows V_{oc} variation with the metal back contact work function (Φ_m). V_{oc} response appears stratified into several stages, in which V_{oc} increases gradually as the work function increases between 4.6 and 5.1 eV. It is also quasi-stable from 5.1 eV to 6 eV. This result could be attributed to the sensitivity of V_{oc} to the barrier height, as proposed in [20]. As the metal work function rises, the Schottky barrier height increases between the metal contact and Si. A greater Schottky barrier height reduces the effective built-in voltage, decreasing V_{oc}. Hence, a poor choice of work function can lead to increased recombination losses at the metal–semiconductor interface, which reduces the number of carriers contributing to V_{oc}. A suitable work function (>5 eV) minimizes these losses, maximizing V_{oc}.

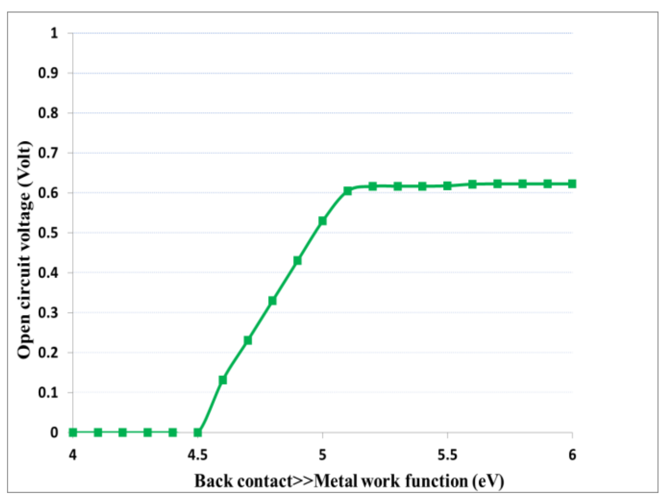

Figure 5. Effect of the back contact work function on Voc of the AlGaN/CdS/Si solar cell

Figure (6) shows the FF variation with the back contact work function. The curve illustrates about zero FF value at low Φm, which suddenly starts to increase at Φm =4.5 eV and becomes almost stable at Φ_m> 5 eV.

FF% of a solar cell is significantly affected by the barrier created by the metal contact. A higher barrier (at low Φ_m connected with the p-type side) increases the difficulty for charge carriers to move across the junction, leading to increased series resistance and reduced current flow. High series resistance, often caused by poor metal–semiconductor contact or high barrier height, leads to significant voltage drops within the cell. This effect reduces the output voltage. This condition results in a lower FF% due to higher voltage drop and energy dissipation at the junction. Moreover, the crated barrier can introduce surface states that act as recombination centers. High recombination rates at the metal–semiconductor interface reduce the number of charge carriers contributing to the current, decreasing FF. Proper selection of metals with high work functions (> 5 eV) as back contact to Si can enhance charge carrier collection and reduce losses, resulting in elevated fill factors and improved solar cell performance [22].

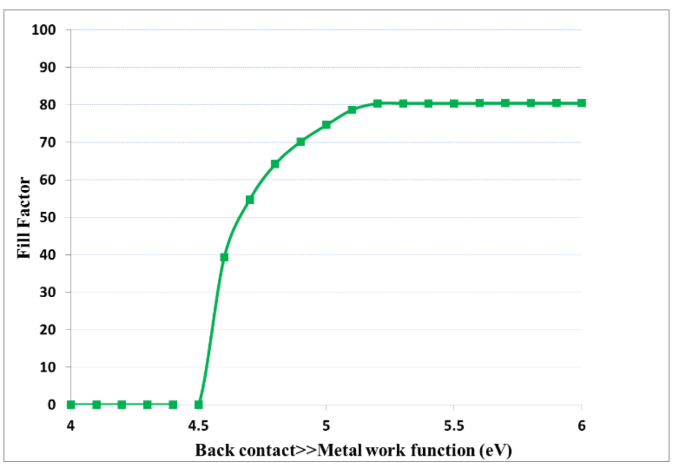

Figure 6. Effect of the back contact work function on FF of the AlGaN/CdS/Si solar cell

Figure (7) illustrates the variation in solar cell efficiency with the metal back contact work function (Φm). The efficiency rises in the range of Φm from 4.5 eV to 5 eV, corresponding to Jsc, Voc, and FF increases, enhancing efficiency. In particular, the efficiency of the solar cell significantly increases, reaching 18.92% at a metal work function of ≈5.2 eV. Beyond Φm >5 eV, the efficiency becomes nearly stable. Accordingly, η has the same trend, given that it is related to these three factors.

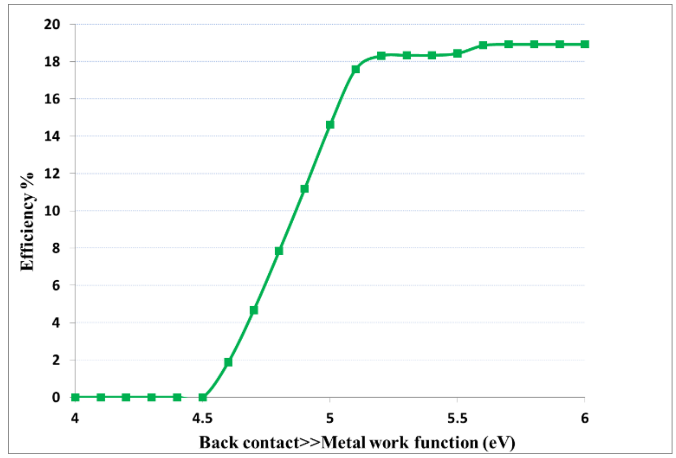

Figure 7. Effect of the back contact work function on η of the AlGaN/CdS/Si solar cell

Conclusions

PL results confirmed the presence of distinct absorption peaks within the visible region for the CdS layer, while the AlGaN samples exhibited characteristic absorption peaks in the UV range. This broad coverage across the electromagnetic radiation spectrum significantly enhances the performance of solar cells. Additionally, this study found that the work function of back contact metals highly affects the solar cell characteristics, including Voc, Jsc, FF%, and η. Metals with high work functions greater than 5.06 eV (such as Au, Pt, and Pd) are recommended to use as back contact to p-type Si for optimal efficiency. The metal work function plays a critical role in solar cell performance, highlighting the importance of proper metal contact to achieve high efficiency, contributing to the advancement of solar cell technology.

Acknowledgments

The authors would like to thank the University of Anbar, Iraq for its support to the work.

Conflict of Interest

The authors confirm that there are no potential conflicts of interest.

References

[1] Ukoba, O., F. Inambao, and A.J.E.P. Eloka-Eboka, *Influence of annealing on properties of spray deposited nickel oxide films for solar cells.* 2017. **142**: p. 244-252.

[2] Mouchou, R., et al., *Numerical simulation and optimization of p-NiO/n-TiO2 solar cell system using SCAPS.* 2021. **38**: p. 835-841.

[3] Ebhota, W., P.Y.J.I.J.o.E.E. Tabakov, and Policy, *Hydropower potentials and effects of poor manufacturing infrastructure on small hydropower development in Sub-Saharan Africa.* 2017. **7**(5): p. 60-67.

[4] Chen, F., et al., *Recent progress in group III-nitride nanostructures: From materials to applications.* 2020. **142**: p. 100578.

[5] Ding, X., et al., *A review of gallium nitride power device and its applications in motor drive.* 2019. **3**(1): p. 54-64.

[6] Taniyasu, Y. and M.J.N.T.R. Kasu, *Improved emission efficiency of 210-nm deep-ultraviolet aluminum nitride light-emitting diode.* 2010. **8**(8): p. 5.

[7] Pandey, A., et al., *Growth, structural and electrical properties of AlN/Si (111) for futuristic MEMS applications.* 2021. **123**: p. 105567.

[8] Zhao, S., et al., *Aluminum nitride nanowire light emitting diodes: Breaking the fundamental bottleneck of deep ultraviolet light sources.* 2015. **5**(1): p. 8332.

[9] Conti III, C.R., J.R. McBride, and G.F.J.T.J.o.P.C.C. Strouse, *Examining the effect of dopant ionic radius on plasmonic M: ZnO nanocrystals (M= Al3+, Ga3+, In3+).* 2021. **125**(14): p. 7772-7779.

[10] Jing, H.X., et al., *Structural and optical properties of AlN/GaN and AlN/AlGaN/GaN thin films on silicon substrate prepared by plasma assisted molecular beam epitaxy (MBE).* 2019. **12**: p. 1177-1181.

[11] Carrano, J., et al., *Very high-speed metal-semiconductor-metal ultraviolet photodetectors fabricated on GaN.* 1998. **73**(17): p. 2405-2407.

[12] Walker, D., et al., *High-speed, low-noise metal–semiconductor–metal ultraviolet photodetectors based on GaN.* 1999. **74**(5): p. 762-764.

[13] Shekari, L., et al., *High-quality GaN nanowires grown on Si and porous silicon by thermal evaporation.* 2012. **263**: p. 50-53.

[14] Khoshsirat, N. and N.A.M. Yunus. *Numerical simulation of CIGS thin film solar cells using SCAPS-1D.* in *2013 IEEE Conference on Sustainable Utilization and Development in Engineering and Technology (CSUDET).* 2013. IEEE.

[15] Burgelman, M., P. Nollet, and S.J.T.s.f. Degrave, *Modelling polycrystalline semiconductor solar cells.* 2000. **361**: p. 527-532.

[16] Movla, H., *Optimization of the CIGS based thin film solar cells: Numerical simulation and analysis.* Optik, 2014. **125**(1): p. 67-70.

[17] Atourki, L., et al., *Numerical study of thin films CIGS bilayer solar cells using SCAPS.* Materials Today: Proceedings, 2016. **3**(7): p. 2570-2577.

[18] Cheung, S. and N.J.A.p.l. Cheung, *Extraction of Schottky diode parameters from forward current-voltage characteristics.* 1986. **49**(2): p. 85-87.

[19] Miao, J., et al., *Recent progress in contact engineering of field-effect transistor based on two-dimensional materials.* 2022. **12**(21): p. 3845.

[20] Hussain, B., et al., *Electron affinity and bandgap optimization of zinc oxide for improved performance of ZnO/Si heterojunction solar cell using PC1D simulations.* 2019. **8**(2): p. 238.

[21] Baliga, B.J., *Fundamentals of power semiconductor devices*. 2010: Springer Science & Business Media.

[22] Demtsu, S. and J.J.T.S.F. Sites, *Effect of back-contact barrier on thin-film CdTe solar cells*. 2006. 510(1-2): p. 320-324.

P- ISSN 1991-8941 E-ISSN 2706-6703 *Journal of University of Anbar for Pure Science (JUAPS)* Open Access
2025,(19), (01):226 – 232

تأثير دالة الشغل للاتصال الخلفي على أداء الخلية الشمسية $Al_{0.1}Ga_{0.9}N/CdS/Si$

بشار محمد صالح، عصمت رمزي عبد الغفور

قسم الفيزياء، كلية العلوم ، جامعة الأنبار ، الأنبار ، العراق
email: alrawi.bashar1@uoanbar.edu.iq

الخلاصة:

في المرحلة الأولى من هذه الدراسة، تم ترسيب طبقة من كبريتيد الكادميوم (CdS) وطبقة من نتريد الألومنيوم والغاليوم (Al0.1GaN0.9) على ركيزة سيليكون باستخدام نظام ترسيب الليزر النبضي (PLD) تمت دراسة الخصائص الفيزيائية للأغشية المحضرة من Al0.1GaN0.9 وCdS. كشفت أطياف التألق الضوئي (PL) عن قمم الانبعاث عند 471 نانومتر لطبقة CdS و339 نانومتر لـــ AlGaN. كانت فجوة الطاقة لطبقة CdS 2.63 إلكترون فولت، بينما كانت فجوات الطاقة لعينات AlGaN 3.66 إلكترون فولت. أظهرت قياسات منحنى I−V لـــ Al0.1GaN0.9 أن ارتفاع الحاجز((ΦB 0.57 إلكترون فولت، بينما بلغت قيم تقارب الإلكترون 4.63 إلكترون فولت. في المرحلة الثانية من هذه الدراسة، تم استخدام نتائج الدراسة التجريبية في المحاكاة الحاسوبية لدراسة تأثير دالة عمل الاتصال الخلفي على أداء الخلية الشمسية AlGaN/CdS/Si وكشفت الدراسة أيضًا أن زيادة دالة عمل المعدن الخلفي أدت إلى تحسين قيم Jsc وVoc، مما أدى إلى تعزيز الكفاءة. زادت كفاءة الخلايا الشمسية بشكل ملحوظ، حيث وصلت إلى 18.92٪ عند دالة عمل معدنية ≈5.2 إلكترون فولت.

الكلمات المفتاحية: AlGaN؛ الخلايا الشمسية؛ دالة الشغل؛ الترسب بالليزر النبضي.